

ACCURACY OF AERODYNAMIC-HEATING PREDICTIONS

By A. L. Nagel and R. A. Hanks
Boeing Airplane Company

INTRODUCTION

L
1
1
1
5
It has been shown in previous discussions that aerodynamic heating has a major role in determining the performance and safety of the Dyna-Soar vehicle. A careful examination of the methods which have been used to calculate aerodynamic heating rates during reentry, and a comparison of those same methods with test data is a necessary part of performance evaluation.

SYMBOLS

D	leading-edge or nose diameter
h	enthalpy
k	conductivity
N_{Pr}	Prandtl number
N_{Le}	Lewis number
p	pressure
q	heat flux
r	radius
R	Reynolds number
T	temperature
u	velocity
x	coordinate
Λ	sweep angle

μ viscosity
 ρ density

Subscripts:

D fraction in dissociation; based on diameter
EXP experimental
e exterior condition
r recovery
s stagnation point or line value
TH theoretical value
w evaluated at wall temperature
 ∞ free-stream value
o stagnation condition

L
1
1
1
1
5

DISCUSSION

The most severe heating rates on winged hypersonic vehicles will occur at the nose and leading edges. The areas involved are relatively small, however, and may admit structural solutions (local cooling or refractories) which are not practical for the remainder of the vehicle. In such a case, the lower-surface material at its most forward point may also become a critical heating point, and may be nearer its temperature limit than either the nose or the leading edge. Other points which would have high local heating rates would be protrusions below the lower surface, such as ventral fins or a dihedral ridge line. Some early Dyna-Soar configurations had such features and were eliminated for that reason. By the end of the Phase I studies, both the Boeing and the Martin-Bell teams had arrived at configurations having simple geometry in regions of high heat transfer. Upper surface complications are less important as the overall heating level for the upper surface is very much lower than for the lower surface. The present Dyna-Soar configuration has only four critical heating points. These are indicated in figure 1 as the nose, the leading edge, the lower surface just aft of the nose, and the dorsal leading edge of the fin, which is critical at low angles of attack.

Complete simulation of the reentry environment is not possible in any of the ground facilities which must be used to provide the bulk of heat-transfer test data. For this reason extrapolation of the test results to the flight condition by some theoretical method is necessary. The study of prediction accuracy cannot be limited to an examination of the data scatter, but must include an evaluation of the theoretical method as well. The combination of a rigorous theoretical approach and test data taken in facilities which simulate the important aspects of the flight environment allows a high degree of confidence in the prediction. In other cases, the theory may be too idealized to lend credence to extrapolations.

Heat-Transfer Equations

The equations used for calculating laminar heating rates both for the reentry condition and for the following comparisons with test data are:

$$q_s = \text{Const.} \frac{\sqrt{\rho_e \mu_e}}{N_{Pr} 0.6} \left(\frac{\rho_w \mu_w}{\rho_e \mu_e} \right)^{0.06} \sqrt{\frac{du_e}{dx}} \left[1 + \left(N_{Le}^{0.52} - 1 \right) \frac{h_D}{h_e} \right] (h_r - h_w) \quad (1)$$

$$q = \frac{q_s}{2} \frac{\left(\frac{p}{p_s} \right) \left(\frac{u_e}{u_\infty} \right) r \sqrt{\frac{u_\infty}{du_e/dx}}}{\left[\int_0^x \left(\frac{p}{p_s} \right) \left(\frac{u_e}{u_\infty} \right) r^2 dx \right]^{1/2}} \quad (2)$$

The constant in equation (1) is 0.793 for the axisymmetric stagnation point and 0.576 for the two-dimensional stagnation line. Equation (2) is used for calculating heat-transfer rates away from the stagnation point. Both equations (1) and (2) are from the work of Kemp, Rose, and Detra, (ref. 1) which is an extension of the earlier work of Fay and Riddell (ref. 2). These equations were selected as a basis for reentry-heating calculations because they are the most rigorously developed methods available, and because they are in good agreement with the test data, as will be shown. The expressions were originally obtained by numerically integrating the boundary-layer equations, using the real-gas equation of state and the Sutherland viscosity law. The cases specifically considered corresponded to the axisymmetric stagnation point, the unswept stagnation line, the flat plate, and a limiting pressure gradient case. Applying simple geometric corrections for flow pattern allows the results to be used for swept leading edges as well.

Calculations by Beckwith (ref. 3) have further shown that equation (1) also results from ideal-gas calculations for both the swept and unswept leading edges except that the Lewis number term is, of course, missing.

The velocity gradient used in applying equation (1) was based on the modified Newtonian pressure distribution, which is within a few percent of the best known values. Equilibrium dissociation was assumed and the values of viscosity calculated by Hansen (ref. 4) were used, and the Lewis number was taken as 1.4. Use of the higher viscosity values has been found to improve agreement with test data. Evaluated in this way heat-transfer rates are 5 to 15 percent higher than those obtained by the method of Fay and Riddell in reference 2.

Since the calculations on which equation (1) is based assumed the Sutherland law for viscosity, use of another viscosity law might appear to invalidate the equation. Recent unpublished calculations of Beckwith and Cohen at the Langley Research Center have shown, however, that the form of the equation does not depend on the viscosity law or even upon the equation of state. It appears then, that use of equation (1) with the best available fluid properties will provide the best estimate of heat transfer.

In the form shown here, the heat-transfer distribution function (eq. (2)) depends only on the local pressure and flow velocity. Simplifying assumptions first suggested by L. Lees (ref. 5) are required to eliminate the dependence on the local transport properties and the pressure gradient. The simplification has been found to be satisfactory for shapes without sharp corners, such as the present Dyna-Soar nose.

In the original development, equation (2) was intended for application to two-dimensional or axisymmetric bodies at zero angle of attack. Application to less simple shapes can be accomplished by replacing the radius terms with an equivalent radius which expresses both the body shape and the streamline pattern which occurs on it.

Equations (1) and (2) supply the required laminar flow heating-rate estimates at all the critical points. At the nose and forward lower surface the Reynolds number is in the range for which laminar-flow heating rates are higher than the turbulent flow rates. The leading edge, however, is limiting in turbulent flow at velocities less than about 19,000 ft/sec. It might appear at first that turbulent flow cannot exist at the leading-edge stagnation line. This is not true for the swept leading edge, as the flow along the stagnation line can become turbulent. The possibility of turbulent low leading-edge heating rates must therefore be considered in aerodynamic heating calculations. The tendency of the boundary-layer secondary flow to

L
1
1
1
1
5

promote transition at very low Reynolds numbers makes it especially important to consider turbulent boundary-layer flow. The expression used to calculate turbulent leading-edge heat transfer for the reentry condition as well as for the comparisons with wind-tunnel data which follow is:

$$q_s = 0.1343 \frac{k_\infty}{D} (R_\infty, D)^{0.8} (N_{Pr})^{1/3} \left(\frac{\mu_w}{\mu_o} \frac{T_\infty}{T_w} \frac{p_e}{p_\infty} \right)^{0.8} \left[\frac{\mu_o}{\mu_\infty} \left(\frac{D}{u_\infty} \frac{du_e}{dx} \right) \right]^{0.2} \times \sin \Lambda^{0.6} (h_r - h_w) \quad (3)$$

This expression was developed by Beckwith and Gallagher (ref. 6). A similar expression can be obtained by applying geometric corrections to turbulent-flow flat-plate theory.

Experimental Comparisons

Stagnation point.- The experimental data for hemispherical stagnation point available for comparison with the theory are presented in figure 2. Data are taken from shock-tube experiments (ref. 7), wind-tunnel tests (ref. 8), and free-flight tests (ref. 9) and have been divided by the theoretical value for the same conditions. A ratio of 1.00 therefore indicates perfect correlation of theory and experiment. The data are shown to scatter from 0.65 to 1.4 times the theory with the average very nearly 1.0 over the entire velocity range. It is believed that this large scatter reflects experimental errors rather than fluctuations in the actual heat-transfer rates. This view is supported by the random nature of the scatter.

The comparison of figure 3 lends further support to this explanation of the scatter. Heat-transfer data from an Atlas (ref. 10) reentry flight are compared with the theory as a function of time. The theory and experimental curves are of similar shape and with almost identical peak values, but with an offset of about 2 seconds in time. If plotted in figure 2, these data would have shown a scatter of about 50 percent around the theoretical curve. The heat-transfer rates shown in figure 3 are calculated from the temperature response of the skin as recorded by thermocouples installed in plugs in the skin. The same characteristic lag of experiment behind theory was observed in many flights. After several other explanations had been ruled out by the consistency of the lag, similar thermocouple installations were calibrated in ground tests. Lags in heating rate were found to occur which, when extrapolated to the flight conditions, are of the same order as those observed in flight. They cannot be said to be precisely the same, as no two thermocouple installations showed exactly the same lag. However, the thermocouple lag does seem to provide a reasonable explanation of the offset. Another

point worth mentioning is in the comparison of the theory of reference 2 with these same data, which is shown to be approximately 10 percent too low at peak heating. Equation (1) was originally selected in preference to the Fay and Riddell theory on the basis of the shock-tube data presented in figure 2. Although both theories fell well within the scatter of the data, the values from the Fay and Riddell method were about 10 percent below the average of the data at high speeds. Re-evaluating the theory to improve the agreement with the average of the shock-tube data brings it into almost exact agreement with the flight data.

Hot-gas radiation heating and variation in wall catalytic effect are two effects not reflected in these data. Calculations based on best available information show that the radiative heat-transfer rate is very small compared to the convective rate for nose radii of 1 foot or less. This result is consistent with the conclusions of previous papers in this conference. The effect of wall catalytic effect may be significantly favorable if nose coating materials can be developed which do not catalyze recombination at the wall. Reductions of over 50 percent are theoretically possible. Neglecting this effect is conservative, and appears to be most realistic at present, as noncatalytic materials have not been developed.

L
1
1
1
5

Laminar distribution.- Nose hemisphere and afterbody data are compared with the theory in figure 4. The agreement is shown to be satisfactory for cones (ref. 11). Recent Langley data on delta wings at angle of attack presented by Bertram and others at this conference are also in good agreement. In making these comparisons equation (2) has been used with an effective radius to correct for nonaxisymmetric shape in the manner previously suggested. This correction requires a knowledge of the streamline patterns as well as the shape of the body. For the cone, the streamline pattern is based on values from the Kopal tables (refs. 12 and 13). For the delta wing, streamline patterns were calculated from a correlation previously made of oil flow patterns obtained in delta wing tests.

Laminar leading edge.- Laminar leading edge data from several wind-tunnel tests (refs. 14 to 16 and unpublished Boeing and Langley test data) are presented in figure 5. The agreement is shown to be excellent over the entire range of sweep angles. None of the experimental leading-edge data shown are in the total temperature range for which real gas effects would be distinguishable. However, the theoretical expression indicates that for the highly swept leading edge the real-gas effect is much smaller than at the stagnation point, and even for that case the predicted (and experimentally supported) effect is only 15 percent at the velocity for maximum reentry heating.

Turbulent leading edge.- Experimental data (ref. 6 and unpublished Boeing test data) for turbulent stagnation-line heat transfer are compared to theoretical values in figure 6. The data are predominantly

below the theory, indicating principally the difficulty of obtaining turbulent flow on the leading edge. The low points at 10° , 20° , and 75° sweep angles are apparently transitional. The low data points taken on delta wing at angles of attack of 30° and 34° are affected by the presence of the wing, which distorts the inviscid flow field. The rest of the data are in very good agreement with the theory.

L
1
1
1
1
5

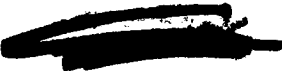
Extrapolation to the flight condition is still somewhat uncertain because the theory has assumed ideal gas relations throughout. Some information regarding the validity of ideal gas heat-transfer calculations in a real gas environment is afforded by an examination of the effect in laminar flow, for which the theory is well developed. Comparisons of ideal-gas solutions for both the stagnation point and the zero pressure gradient flat plate have been found to be within 10 percent of rigorous real-gas solutions at speeds up to satellite velocity. A more significant comparison is presented in figure 7. Experimental turbulent heat-transfer data (refs. 10 and 17 to 20) in the real-gas temperature range are compared with the ideal-gas reference temperature method. The agreement of the theory and experiment is very good over the entire velocity range. The good agreement between the normalized heat transfer in free flight and in the shock tube tends to eliminate the possibility of fortuitous agreement. This agreement also indicates that the shock tube can provide fundamental information about real-gas effects in turbulent flow just as it has been used in the past to study laminar flow stagnation point heat transfer.

CONCLUDING REMARKS

It has been shown that there exists a unified theoretical method for laminar-flow heat transfer which is applicable to critical temperature locations on the Dyna-Soar vehicle. The method rigorously includes real-gas behavior and other phenomena having significant effects on heat transfer. Test data have been presented which confirm the ability of the method to account for such effects over a wide range of conditions.

In the turbulent-flow case no similar well developed theory exists. There is, however, a compensation for this deficiency in the relative insensitivity of the turbulent boundary layer to any influence other than local pressure and velocity. Some turbulent-flow heat-transfer data in the speed range corresponding to reentry maximum heating do exist, and these data are in agreement with semiempirical methods now in use.

From these comparisons it appears that existing methods will satisfactorily predict aerodynamic heating during reentry for the critical locations on the present configuration. Further testing is required to



substantiate this conclusion with the emphasis on data for the configuration specifically chosen. Further testing is also desirable to reduce the uncertainty caused by scatter in available data. These data appear to reflect experimental errors, rather than fluctuations in actual heating rates, so that a design based on these data alone would incorporate unnecessarily large margins in temperature capability, with corresponding weight and performance penalties.

The methods used for theoretical calculations can be extended to other locations on the vehicle. As previously stated, the accuracy of calculations over the rest of the vehicle is less important, as one of the four points discussed will always be nearer its limit temperature. Future alterations of configuration or materials may cause other points to become critical.

L
1
1
1
5



REFERENCES

1. Kemp, Nelson H., Rose, Peter H., and Detra, Ralph W.: Laminar Heat Transfer Around Blunt Bodies in Dissociated Air. Res. Rep. 15, AVCO Res. Lab., May 1958.
2. Fay, J. A., and Riddell, F. R.: Theory of Stagnation Point Heat Transfer in Dissociated Air. Jour. Aero. Sci., vol. 25, no. 2, Feb. 1958, pp. 73-85, 121.
3. Beckwith, Ivan E.: Similar Solutions for the Compressible Boundary Layer on a Yawed Cylinder With Transpiration Cooling. NACA TN 4345, 1958.
4. Hansen, C. Frederick: Approximations for the Thermodynamic and Transport Properties of High-Temperature Air. NACA TN 4150, 1958.
5. Lees, Lester: Laminar Heat Transfer Over Blunt-Nosed Bodies at Hypersonic Flight Speeds. Jet Propulsion, vol. 26, no. 4, Apr. 1956, pp. 259-269.
6. Beckwith, Ivan E., and Gallagher, James J.: Local Heat Transfer and Recovery Temperatures on a Yawed Cylinder at a Mach Number of 4.15 and High Reynolds Numbers. NASA MEMO 2-27-59L, Apr. 1959.
7. Rose, P. H., and Stark, W. I.: Stagnation Point Heat-Transfer Measurements in Dissociated Air. Jour. Aero. Sci., vol. 25, no. 2, Feb. 1958, pp. 86-97.
8. Crawford, Davis H., and McCauley, William D.: Investigation of the Laminar Aerodynamic Heat-Transfer Characteristics of a Hemisphere-Cylinder in the Langley 11-Inch Hypersonic Tunnel at a Mach Number of 6.8. NACA Rep. 1323, 1957. (Supersedes NACA TN 3706.)
9. Pellet, D. M., and Hoshizaki, H.: Summary Analysis of X-17 RTV Program - Aerodynamic Heating and Boundary Layer Transition. Rep. LSMD 2161, Lockheed Aircraft Corp., July 2, 1957.
10. Anon.: Aerothermodynamic Analysis of Mark 2 Flight Test Data - Summary Report. Rep. 59SD743, Sept. 2, 1959.
11. Zakkay, Victor: Pressure and Laminar Heat Transfer Results in Three-Dimensional Hypersonic Flow. WADC TN 182, U.S. Air Force, Sept. 1958.

L
1
1
1
5

12. Staff of the Computing Section, Center of Analysis (Under Direction of Zdeněk Kopal): Tables of Supersonic Flow Around Yawing Cones. Tech. Rep. No. 3 (NOrd Contract No. 9169), M.I.T., 1947.
13. Staff of the Computing Section, Center of Analysis (Under Direction of Zdeněk Kopal): Tables of Supersonic Flow Around Cones at Large Yaw. Tech. Rep. No. 5, M.I.T., 1949.
14. Goodwin, Glen, Creager, Marcus O., and Winkler, Ernest L.: Investigation of Local Heat-Transfer and Pressure Drag Characteristics of a Yawed Circular Cylinder at Supersonic Speeds. NACA RM A55H31, 1956.
15. Feller, William V.: Investigation of Equilibrium Temperatures and Average Laminar Heat-Transfer Coefficients for the Front Half of Swept Circular Cylinders at a Mach Number 6.9. NACA RM L55F08a, 1955.
16. Cunningham, Bernard E., and Kraus, Samuel: Experimental Investigation of the Effect of Yaw on Rates of Heat Transfer to Transverse Circular Cylinders in a 6500-Foot-Per-Second Hypersonic Air Stream. NACA RM A58E19, 1958.
17. Rose, Peter H., Probst, Ronald F., and Adams, Mac C.: Turbulent Heat Transfer Through a Highly Cooled Partially Dissociated Boundary Layer. Res. Rep. 14, AVCO Res. Lab., Jan. 1958.
18. Swanson, Andrew G., and Rumsey, Charles B.: Aerodynamic Heating of a Wing As Determined From a Free-Flight Rocket-Model Test to Mach Number 3.64. NACA RM L56F11a, 1956.
19. Krasnican, M. J., and Wisniewski, R. J.: Free-Flight Determination of Boundary-Layer Transition and Heat Transfer for a Hemisphere-Cylinder at Mach Numbers to 5.6. NACA RM E57F10, 1957.
20. Buglia, James J.: Heat Transfer and Boundary-Layer Transition on a Highly Polished Hemisphere-Cone in Free Flight at Mach Numbers Up to 3.14 and Reynolds Numbers Up to 24×10^6 . NACA RM L57D05, 1957.

L
1
1
1
5

21Y

DYNA-SOAR REENTRY VEHICLE
CRITICAL HEATING LOCATIONS

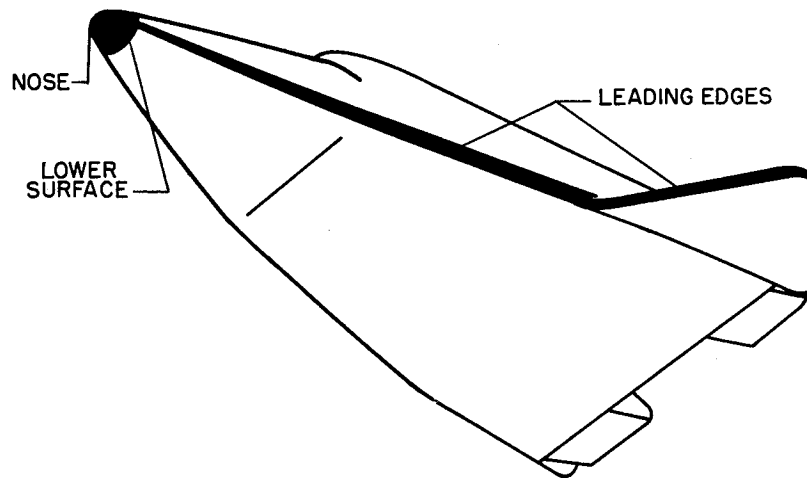


Figure 1

STAGNATION-POINT HEAT TRANSFER

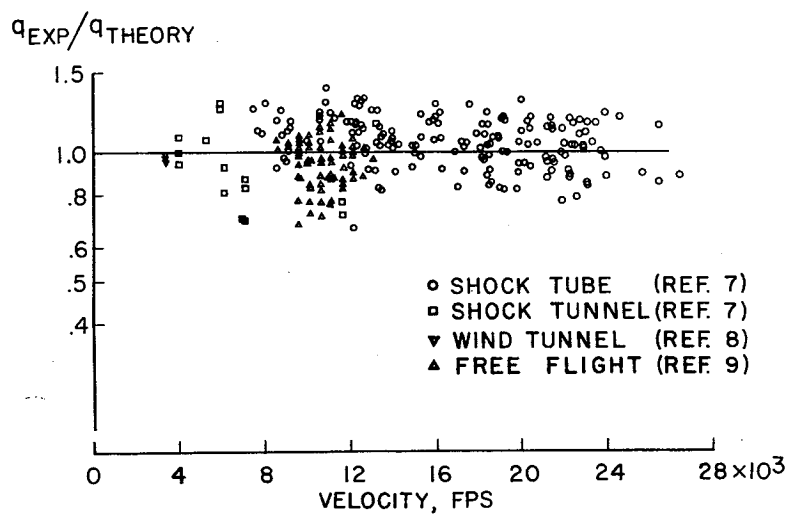


Figure 2

STAGNATION-POINT HEAT TRANSFER
FLIGHT TEST DATA

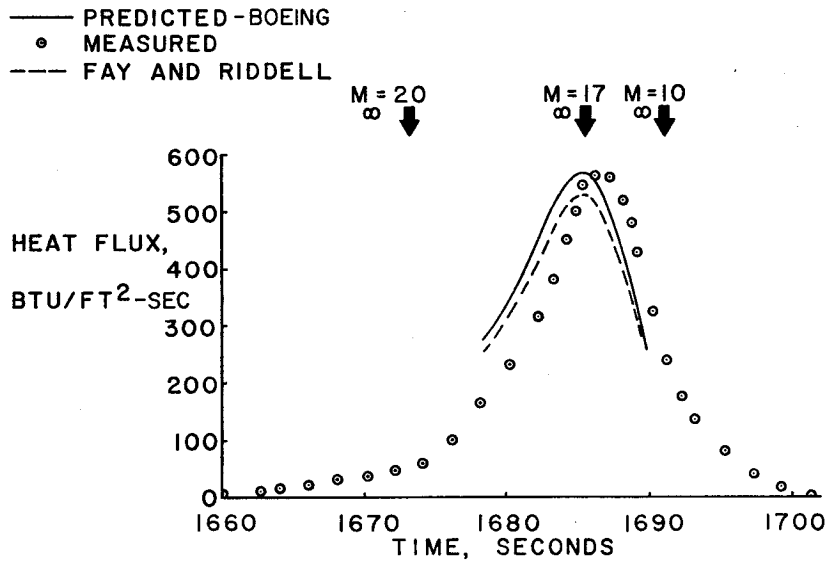


Figure 3

NOSE-AFTERBODY HEAT TRANSFER

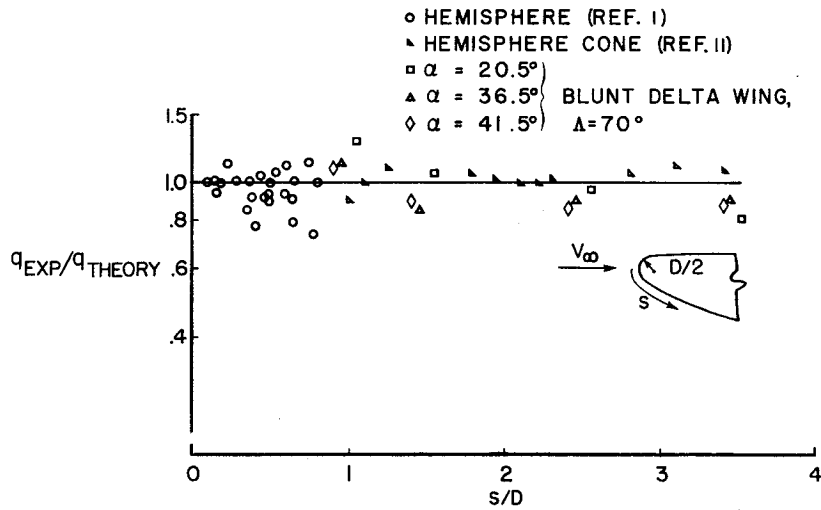


Figure 4

LEADING-EDGE LAMINAR FLOW

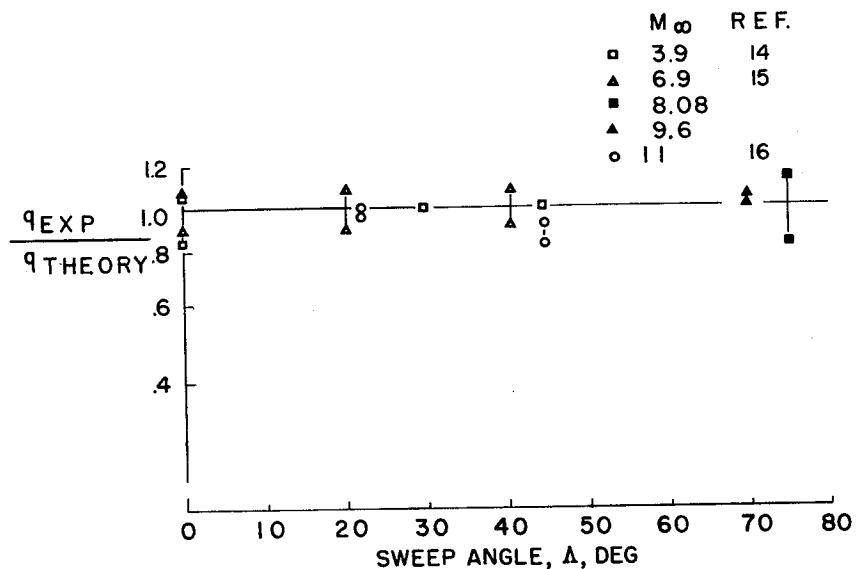


Figure 5

LEADING-EDGE TURBULENT FLOW

○ SWEEP CYLINDER; $R_{\infty, D} = 10^6$; REF. 6

WING L.E.; $\Delta = 75^\circ$; $R_{\infty, D} = 0.75 \times 10^6$; UNPUBLISHED

α , DEG	α , DEG
□ 0	▼ 23
▲ 15	◇ 30
▶ 20	□ 34

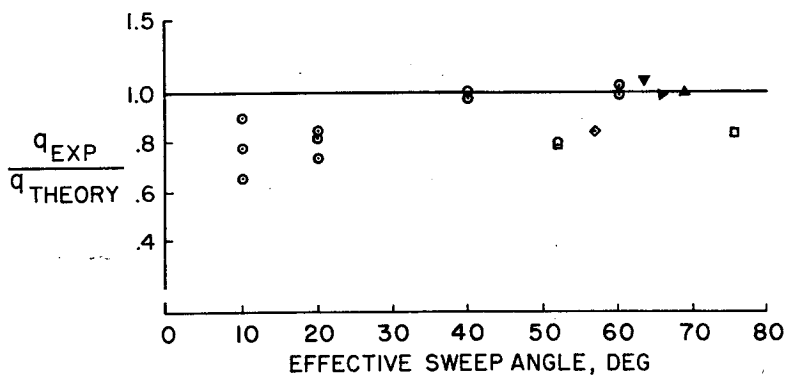


Figure 6

TURBULENT HEAT TRANSFER

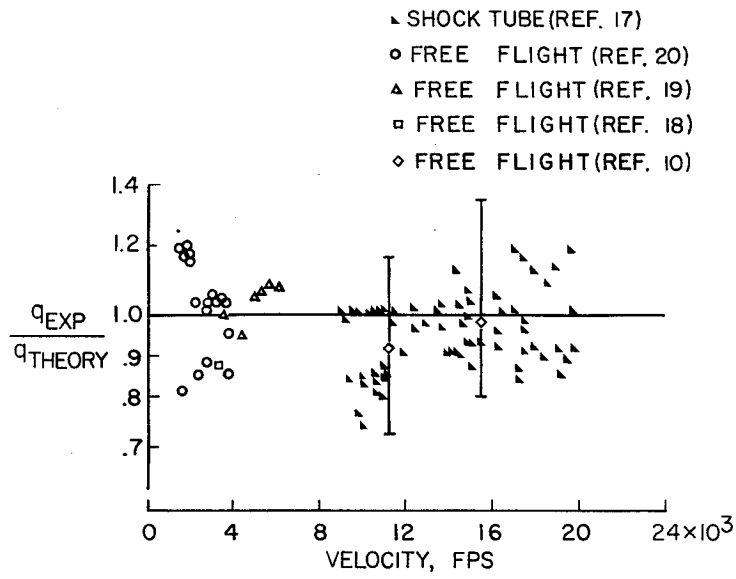


Figure 7